Selective ion-exchange separation of scandium(III) over iron(III) by crystalline alpha-zirconium phosphate platelets under acidic conditions

þÿ A v d i b e g o v i , D ~ e n i t a

2019-05-15

þÿ A v d i b e g o v i , D , Z h a n g , W , X u , J , R e g a d í o , M , K o i v u l a , R & B i n n
Selective ion-exchange separation of scandium(III) over iron(III) by crystalline alpha-zirconium phosphate platelets under acidic conditions ' , Separation and Purification Technology , vol. 215 , pp. 81-90 . https://doi.org/10.1016/j.seppur.2018.12.079

http://hdl.handle.net/10138/323847
https://doi.org/10.1016/j.seppur.2018.12.079

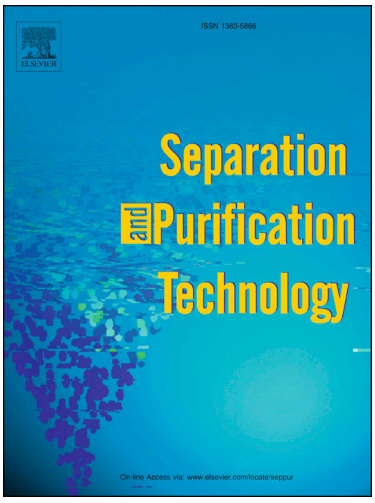

Selective ion-exchange separation of scandium(III) over iron(III) by crystalline α-zirconium phosphate platelets under acidic conditions

Dženita Avdibegović, Wenzhong Zhang, Junhua Xu, Mercedes Regadío, Risto Koivula, Koen Binnemans

PII: S1383-5866(18)33248-9
DOI: https://doi.org/10.1016/j.seppur.2018.12.079
Reference: SEPPUR 15221

To appear in: *Separation and Purification Technology*

Received Date: 17 September 2018
Revised Date: 28 December 2018
Accepted Date: 28 December 2018

Please cite this article as: D. Avdibegović, W. Zhang, J. Xu, M. Regadío, R. Koivula, K. Binnemans, Selective ion-exchange separation of scandium(III) over iron(III) by crystalline α-zirconium phosphate platelets under acidic conditions, *Separation and Purification Technology* (2018), doi: https://doi.org/10.1016/j.seppur.2018.12.079

Selective ion-exchange separation of scandium(III) over iron(III) by crystalline α-zirconium phosphate platelets under acidic conditions

Dženita Avdibegović,[‡a] Wenzhong Zhang,[‡b] Junhua Xu,[b] Mercedes Regadío,[a] Risto Koivula,[b] Koen Binnemans[a*]

[a] Department of Chemistry, KU Leuven, Celestijnenlaan 200F, P.O. Box 2404, BE-3001 Heverlee, Belgium.

[b] Department of Chemistry – Radiochemistry, University of Helsinki, A. I. Virtasen Aukio 1, P.O. Box 55, FI-00014, Helsinki, Finland.

‡ These two authors contributed equally to this work.

*Author to whom correspondence should be addressed:

Email: Koen.Binnemans@kuleuven.be; Phone: +32 16 32 7446

ABSTRACT

A continuous worldwide increase in scandium (Sc) criticality leads to a quest for secondary scandium resources. Among them, bauxite residue (BR) – a waste product from alumina refineries – often contains substantial amounts of scandium. However, the complexity in BR composition drives the need for developing a selective, efficient and cost-effective process to achieve the separation and purification of scandium. Insoluble salts of tetravalent metal ions are inorganic, acid-resistant ion exchangers with well-established preparation procedures, but their potential use in rare-earth recovery and purification has not been extensively explored yet. Zirconium and titanium phosphates, both in amorphous and α-layered crystalline forms, were screened for Sc(III)/Fe(III) separation, as Fe(III) is one of the base elements in BR that is the most challenging to separate from Sc(III). The studied α-zirconium phosphate (α-ZrP, $Zr(HPO_4)_2 \cdot H_2O$) exhibited the highest Sc(III)/Fe(III) separation factors (up to approximately 23) from HCl solutions. The metal selectivity of α-ZrP was considered to be affected by the solution pH, and the size and hydration enthalpy of the metal cations. Breakthrough curves for a binary Sc(III)/Fe(III) solution, composed of metal concentrations realistic to a typical BR leachate, revealed the selectivity of α-ZrP for Sc(III). Furthermore, chromatographic separation of Sc(III) from a real HCl leachate of BR was successfully achieved on an α-ZrP column. After a two-step elution with HCl about 60 % of Sc(III) was collected in fractions without measurable Fe(III), Al(III) or other rare-earth impurities. Overall, this study highlights the possibility for direct and simplified separation of Sc(III) from a much higher concentration of Fe(III) in BR, without the need of using reducing agents.

Keywords: bauxite residue; rare earths; red mud; scandium; titanium phosphate; zirconium phosphate.

1. INTRODUCTION

Scandium (Sc) belongs to the group of rare-earth elements (REEs) which has long been recognised as a valuable commodity for various advanced applications. Currently, the primary use of scandium is in solid-oxide fuel cells (SOFCs) [1]. Scandia-zirconia solid electrolytes can be used at lower temperatures than yttria-stabilised zirconia, because the former has a higher ionic conductivity, resulting in an increased operational stability of SOFCs [2]. Scandium in its metallic form has found applications in aluminium–scandium alloys that are used in aerospace, sports, transportation, and process industries [3–5]. These alloys are much stronger and lighter than other high-strength alloys, exhibit significant grain refinement, strengthen welds and are resistant to corrosion. Besides the bulk applications, addition of scandium compounds to high-pressure lamps renders a light spectrum which is extremely similar to natural sunlight and increases the light output efficiency [6]. Moreover, scandium finds application as host matrix for lasers applied in dentistry [7]. Nevertheless, exploitable scandium-rich minerals and ores are rare [8,9]. Therefore, scandium is usually produced as a by-product of other metal extraction processes. Already in 2014, the European Commission considered scandium as one of the critical raw materials for the European Union, while in 2017 the assessed criticality only increased [10,11]. The lack of primary production mines in Europe imposes a search for secondary resources of scandium and the technologies for extracting scandium from these resources. Bauxites are the primary ores for alumina production through the well-established Bayer process. In Europe, karst bauxites are found more often than their lateritic counterparts, with the former relatively riched in REEs [12]. The REEs from the bauxite are not extracted into the Bayer liquor and are consequently concentrated in the solid waste by a factor of two [12]. The generated solid waste, known as bauxite residue (BR) or red mud, typically contains 50 to 110 mg kg^{-1} of

scandium [12,13]. The scandium content in BR depends on the source of bauxite and the precise processing route. For instance, Greek BR contains even around 120 mg kg^{-1} of scandium [12,13]. This concentration is much higher than the average abundance of scandium in the Earth's crust (22 mg kg^{-1}). Although BR can be considered as a potential scandium resource, other metals are concentrated in BR, especially iron, aluminium, calcium, sodium and titanium, which are energy and process intensive to separate from scandium [13–15]. In principle, scandium can be recovered from a leachate produced by direct leaching of BR with mineral or organic acids, but in this way large amounts of undesired base elements are co-dissolved along with the scandium and other REEs [13,16,17]. Several hydro- and pyrometallurgical processes have been developed to recover the base elements from BR, *i.e.* magnetic separation for iron recovery, smelting of BR to produce pig iron, leaching of BR by organic or inorganic acids (H_2SO_4, HNO_3, HCl, CH_3SO_3H, citric acid, oxalic acid) or alkali roasting for alumina recovery [18–22]. The REEs can then be recovered in a subsequent step from the leachates, but the leachates generated in this way still cannot directly provide REEs compounds of high purity, thus further purification steps are required [21]. The commercial value of REEs depends on their purity. Therefore, it is important to separate them in high purity from the main base elements. Recovery and purification of scandium from BR leachates is generally performed using either solvent extraction, ion-exchange chromatography, precipitation, or a combination of these techniques [9,23–28]. Ion-exchange chromatography has the advantage of high preconcentration factors [29–32]. In BR leachates, the scandium concentration is in the order of several mg L^{-1}, whereas the inevitable impurities of base metals can reach the values of thousands of mg L^{-1} [24]. Iron is one of the base elements that is predominantly present in the BR leachates and is often co-extracted along with scandium [26]. In ion-exchange processes, Sc(III) and Fe(III)

separation from bauxite residue leachates can be challenging because of the same charge of these ions and closer values of hydration enthalpies, in comparison with, for instance, Al(III) ions [25,27,33–35]. One way to tackle the issue of iron impurities is by reducing iron from its trivalent to divalent state. Divalent iron has a much lower charge density than trivalent iron and is therefore easier to separate from trivalent scandium, for instance by solvent extraction with acidic extractants or by use of ion exchangers [27]. However, this reduction step makes the process more costly. Ochsenkühn-Petropulu *et al.* purified scandium from the BR leachate in a Dowex® 5OW-X8 column by eluting first the base elements with 1.75 mol L^{-1} HCl [26]. Scandium and other REEs were subsequently eluted with 6 mol L^{-1} HCl. Nonetheless, separation of scandium from other REEs involved an additional solvent extraction step with di(2-ethylhexyl)phosphoric acid (D2EHPA). It appears that finding a scandium-selective sorbent could address the issue of its recovery and purification from dilute, yet complex solutions like BR leachates.

Insoluble salts of tetravalent metal ions have been extensively studied as ion exchangers with high sorption capacities and good acid, temperature and radiation resistance [36]. They can be prepared in crystalline layered forms, rendering them excellent as hosts for intercalation of a variety of guest molecules and for the synthesis of hybrid materials [37–41]. α-$Zr(HPO_4)_2 \cdot H_2O$ (α-ZrP, with $P2_1/n$ space group) is an established inorganic ion-exchange material of the class metal(IV) phosphates, and has been used in the separation of metal ions, especially for radionuclide removal [42,43]. α-ZrP shows a high sorption capacity (*e.g.* 6.64 meq g^{-1} of exchanger or 2.21 mmol g^{-1} for pure trivalent ion-exchange) [44,45]. The crystal structure of α-ZrP is layered and each layer consists of zirconium atoms lying in a plane and bridged by phosphate groups situated above and below the plane [45]. Although α-ZrP has been investigated

to some extent for the separation of lanthanides, its interesting properties have not been completely explored for the uptake and separation of scandium [46].

As a need for new scandium sources exists, a simple and efficient procedure for the challenging Sc/Fe separation from sources such as BR is required. In the present work, Sc(III) and Fe(III) separation by α-ZrP was investigated in detail. In order to assess and compare the selectivity of the same class of ion exchangers and to reveal the origin of difference in their selectivity, amorphous zirconium and titanium phosphate (am-ZrP, am-TiP) and crystalline titanium phosphate (α-$Ti(HPO_4)_2 \cdot H_2O$ or α-TiP) were screened as well.

2. EXPERIMENTAL

2.1 Chemicals

$ZrOCl_2 \cdot xH_2O$ (> 99.9%, Alfa Aesar, Karlsruhe, Germany), $TiCl_4$ (> 99.9%, Sigma-Aldrich, Helsinki, Finland) and H_3PO_4 (85%, Ashland Chemicals, Columbus, USA) were used for synthesis of sorbents. HNO_3 (65%) and standard solutions of scandium, yttrium, neodymium, dysprosium, lanthanum, aluminium, iron, titanium, silicium, cerium, zirconium and calcium (1000 μg mL^{-1}) from Chem-Lab NV (Zedelgem, Belgium), NaCl (> 99.5%, Fisher Scientific, Loughborough, United Kingdom), HCl (37%, VWR, Leuven, Belgium), Sc_2O_3 (99.99%, kindly provided by Solvay, La Rochelle, France), hydrated $ScCl_3$ (prepared by dissolving Sc_2O_3 in concentrated HCl) and anhydrous $FeCl_3$ (98%) (Acros Organics, Geel, Belgium) were used for solution preparation. Greek BR was kindly provided by Aluminium of Greece (Agios Nikolaos, Greece).

2.2 Equipment

X-ray powder diffraction (XRD) patterns were collected at 2θ angles ranging from 5° to 35° in the Bragg-Brentano geometry on a Bruker D2 PHASER X-ray diffractometer equipped with a CuKα radiation source operating at a voltage of 45 kV and a current of 30 mA. Solid-state ^{31}P magic angle spinning (MAS) nuclear magnetic resonance (NMR) spectra were recorded on a Bruker Advance III 500 MHz spectrometer equipped with a 4 mm H/X/Y MAS probe. The samples were packed in a 4-mm zirconia rotor and spun at a MAS rate of 12 kHz. The spectra were acquired with a 90° pulse (77 kHz RF), a 100 s recycle delay and 64 scans. The ^{31}P chemical shifts were referred to 85% H_3PO_4 (at 0 ppm). The morphology of the platelets was observed by a Hitachi S4800 field emission-scanning electron microscope (FE-SEM) after the sample was sputter-coated with a 3-nm layer of Au-Pd alloy. Batch sorption experiments were performed at room temperature on a VWR International water bath shaker (Type 462-0355). Eppendorf Centrifuge 5804 was used for phase disengagement. A fraction collector CF-2 (Spectrum Laboratories, Inc.) equipped with drop sensor and IPC 8-channel peristaltic pump (ISMATEC) was used for sampling during the chromatography studies. An inductively coupled plasma - optical emission spectrometer (ICP-OES) (Perkin Elmer OPTIMA 8300) was used to measure concentrations of elements in the solutions. The following spectral lines were used for quantification (wavelengths in nm): Al 308.215, Ca 317.933, Ce 413.762, Dy 394.468, Fe 238.204, La 408.672, Nd 401.225, Sc 361.383, Si 251.611, Ti 334.940, Y 371.029.

2.3 Synthesis of metal(IV) phosphate inorganic ion exchangers

α-ZrP was prepared by a reflux method [47]. In summary, 200 mL of 0.5 mol L^{-1} $ZrOCl_2$ was added dropwise to 200 mL of 6 mol L^{-1} H_3PO_4 and refluxed for 48 h at 94 °C. The product was rinsed with water, centrifuged and air-dried at 70 °C overnight.

A hydrothermal synthesis method was used to synthesise α-TiP [27]. An amount of 10 mL of $TiCl_4$ was added dropwise into 50 mL of water with magnetic stirring (300 rpm) until the solution became transparent, and 40 mL of concentrated H_3PO_4 was added. The mixture was heated at 180 °C in a PTFE-lined stainless autoclave for 12 h. The product was filtered, washed with water until a pH of 3.5 was reached, and then air-dried at 70 °C overnight.

The precipitation method was used for the synthesis of am-ZrP and am-TiP [27,48]. In summary, 30.7 g of $ZrCl_4$ or 25 g of $TiCl_4$ was added quickly to 430 mL of 2 mol L^{-1} HCl solution under magnetic stirring (300 rpm) until it gave a totally transparent solution. The prepared solution was added dropwise into 400 mL of 1.25 mol L^{-1} H_3PO_4 solution while stirring at 150 rpm. The resulting white solid was allowed to stand in the mother solution for 24 h before filtering out. The am-ZrP was subsequently washed with 2 mol L^{-1} H_3PO_4, 1 mol L^{-1} HNO_3 and with water until a pH of 3.0 was reached. The am-TiP was washed only with water until the pH of 3.5 was attained. The products were then air-dried at 70 °C overnight.

2.4 Batch sorption studies

Typically, 0.050±0.001 g of the ion exchanger was placed in a 20 mL glass vial and 20 mL of synthetic feed solution of Sc(III) and/or Fe(III) with pre-adjusted pH was added. Unless

otherwise specified, concentrations of Sc(III) and Fe(III) were 1.0 mmol L^{-1}, the shaking speed was 300 rpm and the equilibration time was 18 h. The experiments were carried out at room temperature in HCl media. The uptake of Sc(III) and Fe(III) from a 3 mol L^{-1} NaCl solution was investigated under the same experimental conditions. After equilibration, the samples were filtered through 0.20 μm PVDF syringe filters. The filtrate was then diluted to a concentration suitable for ICP-OES analysis. The reusability of α-ZrP for Sc(III) uptake was examined by repeating the sorption-desorption steps three times. α-ZrP was equilibrated with 20 mL of Sc(III) solution (initial pH, pH_{ini} = 1.6), centrifuged for 15 min at 2880 *g* and the supernatant was taken by a pipette. Then, α-ZrP was washed two times with 10 mL of ultrapure water, centrifuged and dried for 2 h at 50 °C in a vacuum oven, before 20 mL of an equimolar 1.5 mol L^{-1} HNO_3 and H_3PO_4 mixture was introduced for Sc(III) desorption. Desorption experiments were conducted for 24 h at the same shaking conditions as for the uptake experiments.

The amount of the metal ions sorbed onto the ion exchangers q (mmol g^{-1} of dry ion exchanger) was calculated from eq 1:

$$q = \frac{(c_{ini} - c_{eq}) \cdot V}{m} \qquad \text{(eq 1)}$$

The initial metal ion concentration in the solution (mmol L^{-1}) is c_{ini}, the equilibrium concentration of metal ions in the solution (mmol L^{-1}) is c_{eq}, V is the volume of the solution (L) and m is the mass of a dry ion exchanger (g).

The metal uptake can also be quantified by the distribution coefficient (K_D), following eq 2:

$$K_D = \frac{q}{c_{eq}} \qquad \text{(eq 2)}$$

K_D is the ratio of the sorbed amount of metal divided by its concentration in solution at equilibrium (L g^{-1}).

The separation factor ($\alpha_{A/B}$) is then defined as the ratio of the distribution coefficient of two metals A and B (eq 3).

$$\alpha_{A/B} = \frac{K_{D_A}}{K_{D_B}} \quad (K_{D_A} \geq K_{D_B}) \qquad \text{(eq 3)}$$

2.5 Column chromatography sorption studies and bauxite residue leaching

A low-pressure vertical glass column (BIO-RAD) of 10 cm length with an inner diameter of 1 cm was used in chromatography separation experiments. A slurry with 1.0 g of α-ZrP and 10 mL of a 1 mol L^{-1} NaCl solution was prepared and the column was packed to a bed volume (*BV*) of approximately 2.0 mL (the total volume of the α-ZrP together with the void volume in the column). The remaining NaCl impurities were washed by pumping through 5 *BV* of 1.5 mol L^{-1} HCl. α-ZrP was pre-conditioned with HCl solution of pH = 0.8 prior to the breakthrough curve experiments and pH = 2.2 prior to elution studies with the HCl BR leachate. The breakthrough curves were constructed by pumping the binary solution of 0.04 mmol L^{-1} Sc(III) and 1.72 mmol L^{-1} Fe(III), with pH_{ini} of 0.8, through the α-ZrP column. All column chromatography experiments were conducted at room temperature and a flow rate of 2 mL h^{-1}. The fractions collected after elution were analysed by ICP-OES.

The leaching of Greek BR (Agios Nikolaos, Greece) was performed as described elsewhere [13]. In summary, BR was air-dried for 20 h at 105 °C in an oven. An aliquot of 100.0 mL of

0.7 mol L^{-1} HCl was added to 10.0 g of BR. The mixture was shaken for 6 h on a rotary mixer at 60 rpm and at room temperature. The leachate was filtered through a 0.20 μm PVDF syringe filter and 5.0 mL of the freshly prepared leachate was used for a chromatographic separation experiment with pH_{ini} = 2.2, without any further treatment.

The recovery of elements from the BR leachate by the α-ZrP column was calculated by applying eq 4:

$$Recovery\ (\%) = \frac{c_L - c}{c_L} \cdot 100 \qquad \text{(eq 4)}$$

where c_L (mmol L^{-1}) is the initial concentration of elements in the BR leachate, and c (mmol L^{-1}) is the concentration of elements in the fractions collected after the uptake by the α-ZrP.

3. RESULTS AND DISCUSSION

3.1 Characterisation of α-ZrP

The characterisations of am-ZrP, am-TiP and α-TiP were reported in our previous studies [27,48]. Moreover, the synthesised α-ZrP platelets have been extensively studied and characterised in the literature [49,50]. As the focus of the present study falls on the metal separation behaviour, only typical characterisations to check the purity of the obtained α-ZrP platelets were run. The XRD patterns (Figure 1) showed typical peaks for the α-ZrP phase, with the peak at around 11.8° (2θ) being the most intense. This peak represents the diffraction from the (002) plane and hence indicates the interlayer distance of the α-ZrP at 7.6 Å [46,51]. According to the formula of α-ZrP ($Zr(HPO_4)_2 \cdot H_2O$), only one kind of phosphate group should

be present, which can serve as an indicator for the material purity. The solid-state ^{31}P MAS NMR spectrum (Figure 2) of the α-ZrP platelets appears with only one dominant peak (-18.4 ppm) with two shoulders (-16.8 and -20.3 ppm) within the ^{31}P chemical shift region of $–HPO_4$ groups. It was reported that the dominating peak could be assigned to the $–HPO_4$ groups of the interlayer, while the shoulders could be assigned to the phosphate groups on the edges of the platelet (with possible partial hydrolysis and dehydration) [47,52]. The absence of a resonance peak at 0 ppm indicated that no residual H_3PO_4 was left behind in the material. Morphologically speaking, the α-ZrP particles are highly ordered hexagonal platelets with a diameter of approximately 3 μm, as shown by the SEM images (Figure 3).

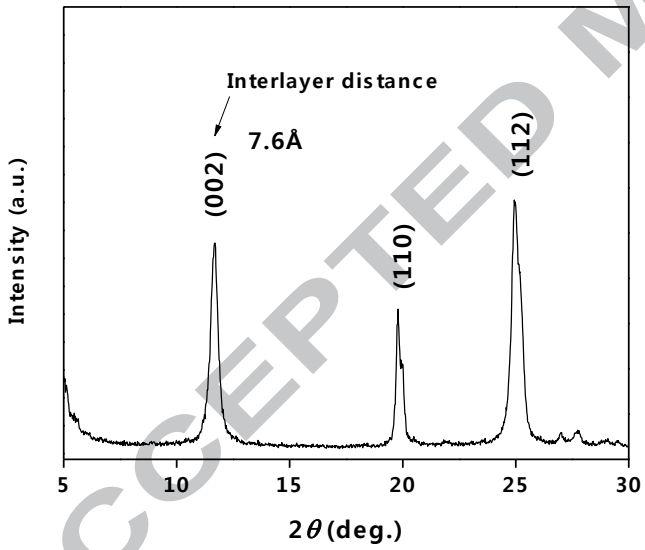

Figure 1. XRD patterns of the synthesised α-ZrP platelets.

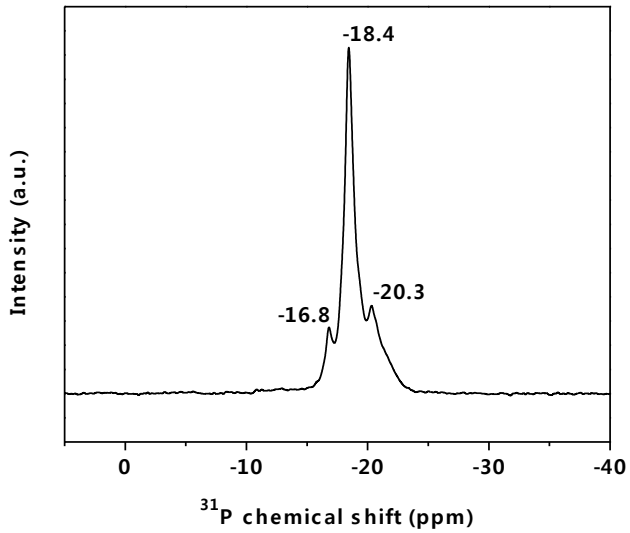

Figure 2. Solid-state ^{31}P MAS NMR spectrum of the synthesised α-ZrP platelets.

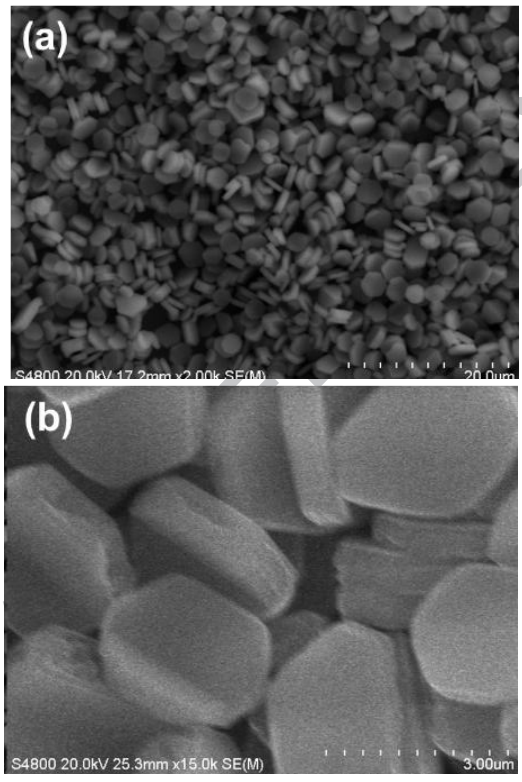

Figure 3. SEM micrographs of the synthesised α-ZrP platelets at different magnifications: (a) 2000× and (b) 15000×.

3.2 Selectivity of metal(IV) phosphate inorganic ion exchangers

ZrP and TiP are widely investigated metal(IV) phosphates that can be obtained in the metal(IV)–H_3PO_4 system. In the present study, their amorphous and crystal forms (am-ZrP, am-TiP, α-ZrP and α-TiP) have been investigated for the separation of Sc(III) and Fe(III) from acidic media (Figure 4). Both amorphous and crystalline TiP and ZrP exhibited the preferential uptake of Sc(III) over Fe(III). This selectivity for Sc(III) might be explained by the lower hydration enthalpy of Sc(III) than that of Fe(III), as less energy is required to dehydrate Sc(III) when occupying the ion-exchange sites [34,53]. Although the amorphous forms of ion exchangers exhibited a higher uptake capacity for both Sc(III) and Fe(III) (especially am-ZrP), α-ZrP exhibited the highest Sc(III)/Fe(III) separation factors (Figure 4). It should be noted that the separation factors obtained in the batch sorption studies provide limited information about the separation capability of the sorbent, and the separation between metal ions can be further enhanced by, for instance, column chromatography.

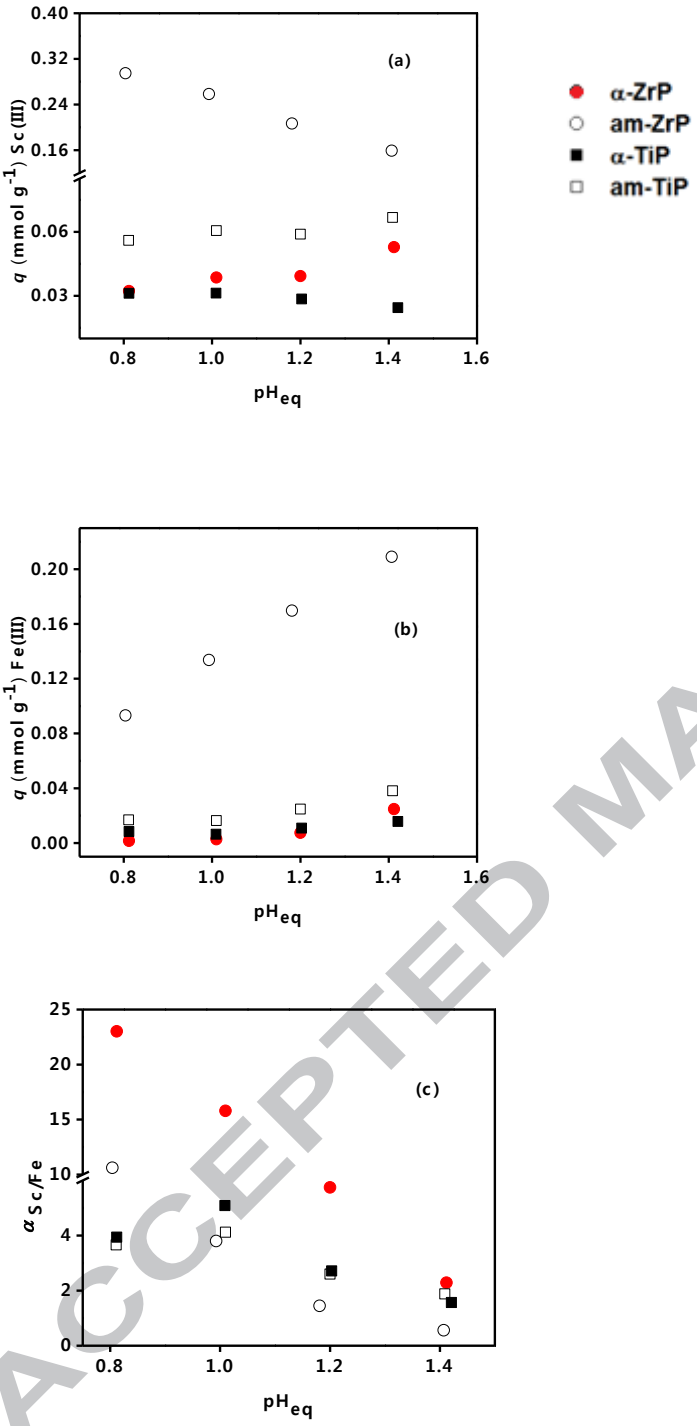

Figure 4. Sc(III) (a) and Fe(III) (b) uptake (q) and separation factors (α) (c) as a function of pH_{eq} with different inorganic ion exchangers. Feed: binary equimolar solutions c_{ini} = 0.9 mmol L^{-1}, V = 20 mL. m = 0.050 g, 300 rpm, room temperature.

Besides the superior selectivity of α-ZrP over am-ZrP for Sc(III), the crystalline form is also highly preferred over the amorphous form for reproducible performance, and it is more stable over a wide pH range. With the increase in pH a general decrease in separation factors was observed, presumably as a consequence of the increase in the availability of ion-exchange sites, which resulted in an elevated Fe(III) uptake. Ion-exchange properties of metal(IV) phosphates depend on the central atom and their crystalline structure [54]. Based on the lattice radius of 6-coordinate Ti(IV) (0.74 Å) and Zr(IV) (0.86 Å), and the high polarising power of Ti(IV), it might be assumed that the acidity of the phosphate group in α-TiP is higher than in α-ZrP [53]. Still, α-ZrP possesses a bigger free area around the phosphate group (24.0 $Å^2$) than α-TiP (21.6 $Å^2$), indicating that there is more available cavity around the exchange sites for guest species [54], [55]. The phosphate groups in ZrPs are believed to have a greater mobility compared to those in TiPs, because the lesser covalent nature of the Zr–O bonds with regards to the Ti–O bonds. Bigger free area and greater phosphate mobility are both convenient for accommodating larger species, and as the ionic radius of Sc(III) is larger than that of Fe(III), the uptake of Sc(III) is facilitated. The prominent selectivity of α-ZrP is an overall result of different effects: the hydration enthalpy, the pH of solution, and the accessibility of phosphate groups. Based on the above, only α-ZrP was selected for further detailed study.

3.3 pH dependence

The solution pH is one of the crucial parameters that can affect the uptake of metal ions and the selectivity of an ion exchanger. The ion-exchange uptake of metal ions (M^{n+}) on α-ZrP can be expressed using eq 5 (water of crystallisation is omitted for clarity) [41]:

$$Zr(HPO_4)_2 + 2/n\ M^{n+} \leftrightarrows Zr(M_{1/n}PO_4)_2 + 2H^+ \qquad \text{(eq 5)}$$

Obviously, lowering the solution pH would drive the equilibrium towards the left-hand side, resulting in lower metal uptake. The influence of the pH was further investigated from single-element solutions and Sc(III)/Fe(III) binary HCl solutions. As expected, an increase in metal ion uptake was observed as the pH_{eq} increased, both from single and binary solutions (Figure 5). The uptake of Sc(III) was generally more favourable than the uptake of Fe(III). However, the uptake of Sc(III) from acidic media (0.42 mmol g^{-1} from single Sc(III) solution at pH 1.6) was well below the total sorption capacity of α-ZrP reported in the literature (6.64 meq g^{-1} or 2.21 mmol g^{-1} of Sc(III)) [45]. α-ZrP exhibits a diprotic character, with pKa_1 = 3.3 and pKa_2 = 6.3[46]. Since the present sorption systems are operating at pH values far lower than the first acid dissociation constant, the phosphate groups will be fully protonated and the obtained uptake values are expected.

The influence of pH on Sc(III) and Fe(III) uptake by α-ZrP was additionally investigated from 3 mol L^{-1} NaCl solutions. Na(I) ions can act as ion-exchange reaction synergists, by entering the layers of α-ZrP and possibly by expanding the interlayer distance [36]. Na(I) ions can

subsequently be exchanged by highly charged ions like Sc(III) and Fe(III), due to their stronger electrostatic interaction with α-ZrP. Moreover, Fe(III) and Sc(III) can form chloro complexes in the presence of an excess of chloride anions, which affects the charge of metal ions and may alter the selectivity of α-ZrP [42,43]. The total uptake of metal ions was higher from NaCl-containing solutions, which confirmed the synergistic effect of Na(I) in the ion-exchange reaction (Figure 5, Figure 6). However, the increase in the interlayer space of α-ZrP after Na(I) and Sc(III) exchange was not observable in the XRD spectra (Figure 7). At such low pH, a low amount of lattice water was displaced by metal ions, and therefore the change in the distance between the adjacent α-ZrP layers was not possible to detect by powder XRD [49].

Furthermore, in the pH_{eq} region between 1.0 and 1.3, the uptake of Sc(III) from binary solutions decreased, followed by an increase in the uptake of Fe(III) (Figure 6). Na(I) and Fe(III) ion exchange were facilitated by an increase in pH, which presumably hindered Sc(III) exchange. Still, as the pH further increased ($pH_{eq} \approx 1.4$) the uptake of both Sc(III) and Fe(III) from a binary solution increased, as there are generally less H^+ ions competing in the ion-exchange reaction with metal ions. High Sc(III)/Fe(III) separation factors from NaCl solution can therefore only be attributed to the Na(I) synergistic effect.

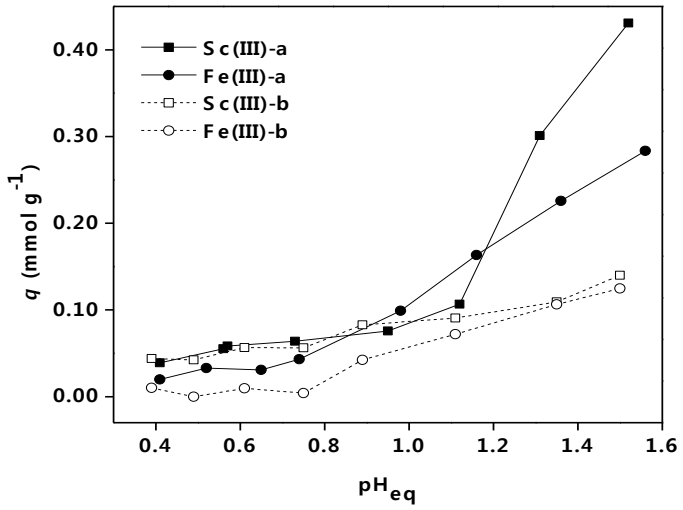

Figure 5. Uptake of Sc(III) and Fe(III) by α-ZrP from HCl solutions of: (a) single-element solutions, and (b) equimolar binary mixture of Sc(III) and Fe(III). Feed: c_{ini} = 1.1 mmol L^{-1}, V = 20 mL. m = 0.050 g. 300 rpm, room temperature.

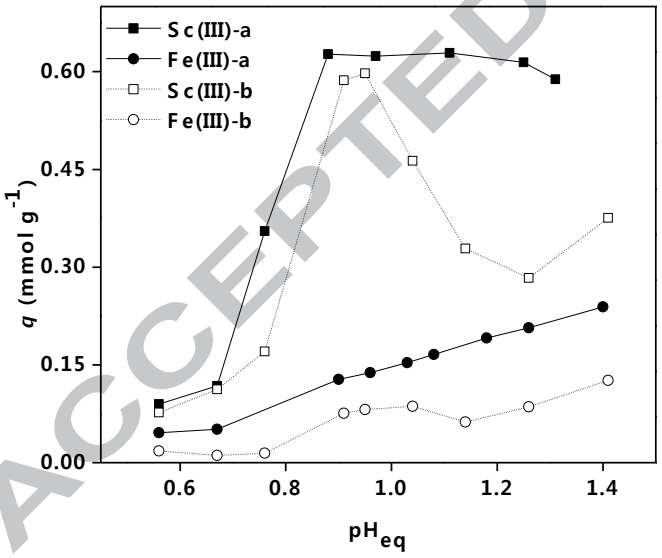

Figure 6. Uptake of Sc(III) and Fe(III) by α-ZrP from HCl solutions with 3 mol L^{-1} NaCl of: (a) single element solutions, and (b) binary solutions. Feed: $c_{ini} \approx$ 1.1 mmol L^{-1}, V = 20 mL. m = 0.050 g. 300 rpm, room temperature.

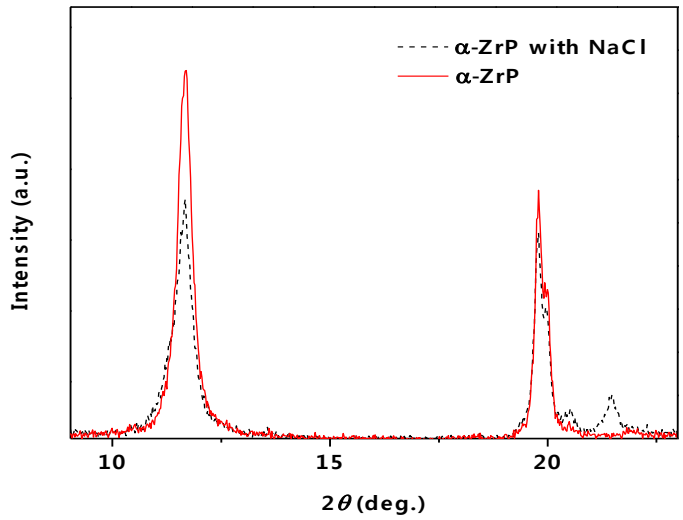

Figure 7. XRD patterns of α-ZrP platelets prior to and after Sc(III) uptake from 3 mol L^{-1} NaCl solution at pH_{eq} = 1.4.

The formation of Fe(III) chloro complexes did not diminish the uptake of Fe(III) by the α-ZrP, as its uptake was even higher from NaCl solutions due to the Na(I) synergistic effect (Figure 6, Figure 8). Only in a narrow pH_{eq} region, the calculated Sc(III)/Fe(III) separation factors from NaCl solutions significantly surpassed the separation factors obtained by the α-ZrP without NaCl addition (Figure 8). Therefore, the incremental selectivity enhancement of α-ZrP for Sc(III) with the addition of NaCl was not further explored. The salt addition would result in a more complex downstream process in practice. Note that the activity coefficient of H^+ in this solution is close to one. Therefore the pH measurement was still reliable in the presence of 3 mol L^{-1} NaCl [56].

To further elucidate the uptake mechanism of Sc(III) and Fe(III) from HCl solutions with and without NaCl, additional studies on α-ZrP with Raman spectroscopy, extended X-ray absorption fine structure (EXAFS) and ^{31}P MAS NMR were attempted. Unfortunately, due to a very low

uptake of Sc(III) and Fe(III) from acidic solutions and small changes in the structure of α-ZrP, the spectra obtained by these techniques were inconclusive and therefore omitted here.

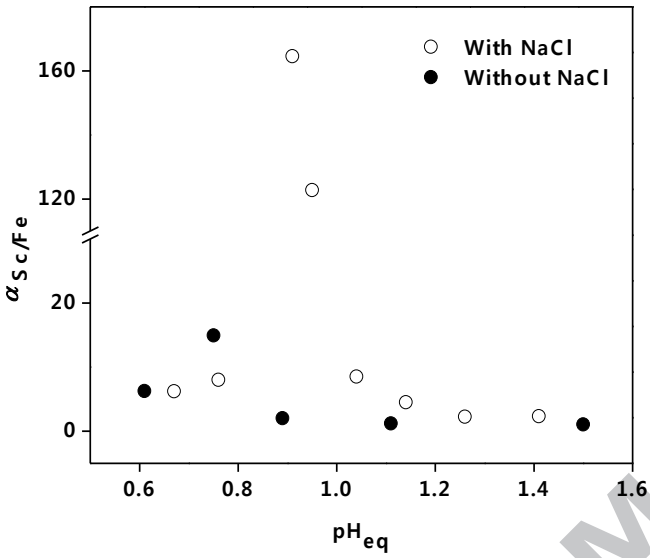

Figure 8. Sc(III)/Fe(III) separation factors (α) with increasing pH_{eq} of Sc(III)/Fe(III) binary solutions with and without 3 mol L^{-1} NaCl. Feed: $c_{ini} \approx 1.1$ mmol L^{-1}, $V = 20$ mL. $m = 0.050$ g. 300 rpm, room temperature.

3.4 Sorption isotherms

The most common and the simple models to describe the sorption of metal ions from aqueous solutions are the empirical Langmuir and Freundlich models. Therefore, the ion exchange of Sc(III) and Fe(III) was investigated from HCl solutions at $pH_{eq} \approx 1.5$ by varying their concentration (Figure 9,

Table 1), and the equilibrium data were fitted to the linearised Langmuir (eq 6) and the Freundlich (eq 7) equations.

$$\frac{c_{eq}}{q} = \frac{1}{K_L \cdot q_m} + \frac{c_{eq}}{q_m} \quad \text{(eq 6)}$$

In the linearised Langmuir equation c_{eq} is the concentration of metal ion at equilibrium (mmol L^{-1}), q is the amount of metal ion sorbed by dry the ion exchanger (mmol g^{-1}), K_L is the Langmuir constant (L $mmol^{-1}$), q_m is the maximum sorption capacity (mmol g^{-1}).

$$\log\ q = \log K_F + \frac{1}{n}\ \log\ c_{eq} \quad \text{(eq 7)}$$

In the linearised Freundlich equation, K_F is the Freundlich isotherm constant and n is the sorption intensity. A plot of log q versus log c_{eq} represents the Freundlich adsorption isotherm at room temperature.

The Langmuir isotherm model described the sorption of Sc(III) better (regression coefficient, R^2 = 0.999) than the Freundlich model (R^2 =0.107) (

Table 1). The high uptake at low Sc(III) concentration indicates a very strong interaction between Sc(III) and α-ZrP. In addition, when the Sc(III) concentration increased, the saturation constant value was approached. Sorption of Fe(III) fitted both Langmuir and Freundlich isotherm models (R^2 of 0.982 and 0.942, respectively). The results suggest that monolayers of Sc(III) and Fe(III) were sorbed on the α-ZrP surface, but the sorption capacity of α-ZrP was higher for Sc(III) than that for Fe(III) (

Table 1). The n value for Fe(III) indicates a high sorption intensity.

Table 1. Langmuir and Freundlich sorption isotherm parameters for Sc(III) and Fe(III).

Isotherm model	Langmuir		Freundlich	
	Sc	Fe	Sc	Fe
Correlation coefficient (R^2)	0.999	0.982	0.107	0.942
Intercept	0.003	0.272	-0.074	-0.402
Slope	1.199	2.347	0.132	0.404
Calculated q_m (mmol g^{-1})	0.83	0.43		
K_L (L $mmol^{-1}$)	468	9		
K_F ($mmol^{1-n}$ g^{-1} L^n)				0.4
n				2.5

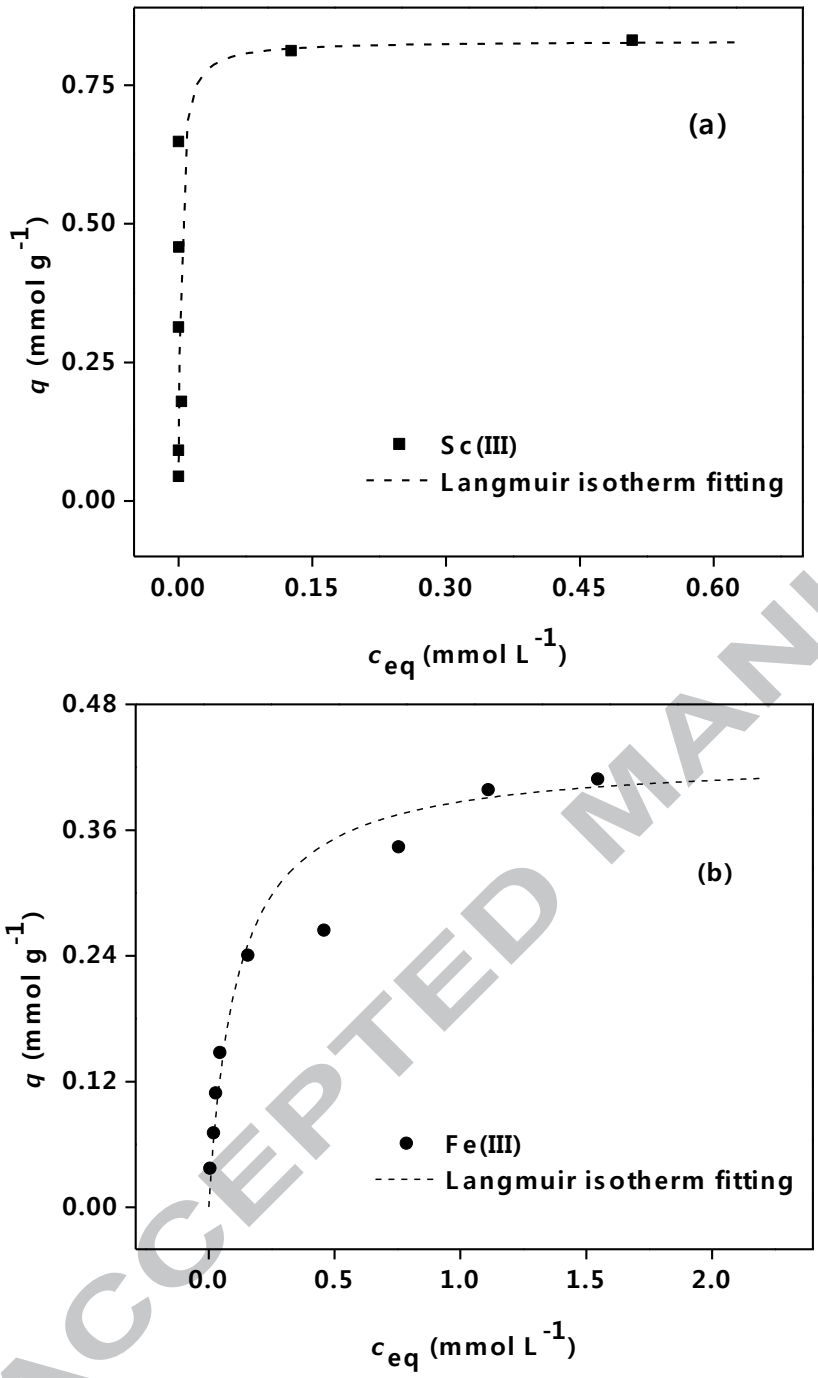

Figure 9. Sorption isotherms for Sc(III) (a) and Fe(III) (b) with α-ZrP. Initial concentration range from 0.1 to 2.6 mmol L^{-1}, $pH_{eq} \approx 1.5$, $m = 0.050$ g, $V = 20$ mL, 300 rpm, room temperature.

Sorption capacities of several sorbents for Sc(III) are given in the Table 2. Although the sorption capacities were determined under different pH, it is evident that even at low pH of 1.5 α-ZrP exhibits a remarkable sorption capacity for Sc(III), superior to other silica- or resin-based sorbents.

Table 2. Sorption capacities (q_m) of several sorbents for Sc(III).

Sorbent	**pH**	q_m **(mmol g^{-1})**	**Reference**
Aminocarbonylmethylglycine-immobilised resin (PA-AG)	3	0.28	[57]
Betainium sulfonyl(trifluoromethanesulfonylimide) poly(styrene-co-divinylbenzene) [Hbet-STFSI-PS-DVB]	3	0.36	[35]
Resin with glycol amic acid group	–	0.36	[58]
Amorphous titanium phosphate (am-TiP)	2	0.54	[27]
Saponified product of orange juice residue	4	0.60	[59]
Lysine modified SBA-15 silica	5	0.79	[60]
α-zirconium phosphate (α-ZrP)	1.5	0.83	Present work

3.5 Kinetic study

The reaction kinetics primarily defines the efficiency of an ion exchanger. To examine the rate-determining step for ion exchange, the widely used pseudo-first-order, pseudo-second-order and intra-particle diffusion kinetic models were applied (eqs 8, 9 and 10).

$$\log (q_m - q_t) = \log q - \frac{k_1}{2.303} \cdot t \qquad \text{(eq 8)}$$

In the linearised pseudo-first-order kinetic model equation, q_m and q_t are the amounts (mmol g^{-1}) of metal ions per amount of ion exchanger (g) at equilibrium and at time t, respectively, k_1 is the pseudo-first-order rate constant (min^{-1}).

$$\frac{t}{q_t} = \frac{1}{k_2 \cdot q_t^2} + \frac{t}{q_m} \qquad \text{(eq 9)}$$

In the linear form of the pseudo-second-order kinetic model equation, k_2 is the pseudo-second-order rate constant (g $mmol^{-1}$ min^{-1}).

$$q_t = k_{int} \cdot t^{\frac{1}{2}} + C \qquad \text{(eq 10)}$$

The intra-particle diffusion rate is obtained by linearisation of the curve $q_t = f(t^{1/2})$. In the intra-particle diffusion equation k_{int} (mmol g^{-1} $h^{1/2}$) is the intra-particle rate constant and C is a constant (mmol g^{-1}) which is proportional to the extent of the boundary layer thickness.

The kinetics of Sc(III) ion exchange by α-ZrP better fitted the pseudo-second-order kinetics model (R^2 = 0.999) (Figure 10,

Table 3) than the pseudo-first-order kinetics model (R^2 = 0.473) or the intra-particle diffusion model (R^2 = 0.809). The results suggest that the chemical reaction at the surface of α-ZrP is the rate-limiting step, rather than diffusion-related phenomena. Sc(III) uptake from HCl media with α-ZrP was remarkably fast and 95% of Sc(III) was exchanged within 15 minutes (Figure 10). The fast kinetics of Sc(III) ion-exchange significantly outstand the previously reported equilibration time of 72 hours for the REEs (neodymium and dysprosium) uptake by the α-ZrP [46]. This indicates the potential for applying this ion exchanger at large-scale, *e.g.* column chromatography separations. Still, when an ion exchanger is packed in a column, additional practical factors affecting the exchange of metal ions must be considered, like the flow rate of feed solution through the column, selectivity coefficient, particle size and operation temperature.

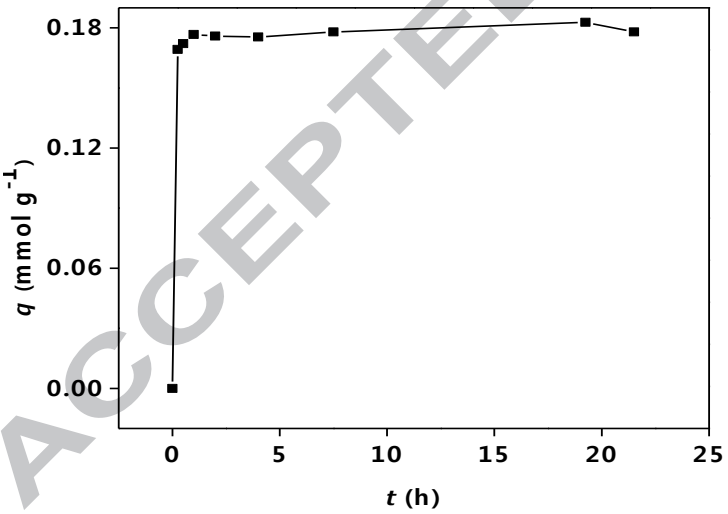

Figure 10. Kinetics of Sc(III) sorption by α-ZrP. Feed: c_{ini} = 0.5 mmol L^{-1}, pH_{eq} = 1.5, m = 0.050 g, V = 20 mL. 300 rpm, room temperature.

Table 3. Parameters calculated from the linear fit of kinetic model equations.

	Pseudo-second-order
Regression coefficient	0.999
Intercept	6.70
Slope	5.62
Calculated q_m (mmol g^{-1})	0.15
k_2 (gmmol min^{-1})	7.99

3.6 Reusability of α-ZrP

Prior to its application in a column chromatography for metal ions separation, the reusability of ion exchanger must be examined. A mixture of HNO_3 and H_3PO_4 was used for desorption of Sc(III), since this acid mixture has already been successfully applied for Sc(III) recovery from am-TiP [27]. As shown in Figure 11, Sc(III) could be quantitatively desorbed from α-ZrP with this acid mixture and α-ZrP could be successfully reused, without any significant decrease in Sc(III) uptake over 3 subsequent adsorption-desorption cycles.

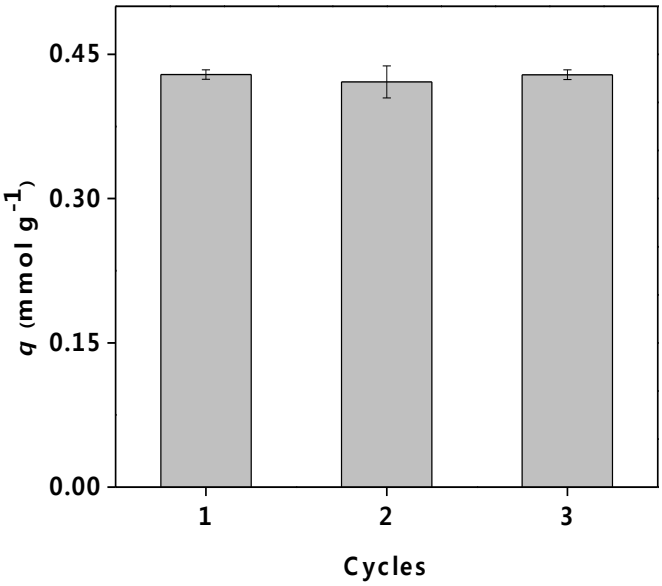

Figure 11. Reusability of α-ZrP (triplicate measurements). Sorption conditions: m = 0.050 g, 20 mL of 1.0 mmol L^{-1} Sc(III), pH_{ini} = 1.6, pH_{eq} = 1.5, 18 hours. Desorption conditions: 20 mL of 1.5 mol L^{-1} equimolar mixture of HNO_3 and H_3PO_4, 24 hours.

3.7 Column chromatography studies

The vital parameters for Sc(III) recovery by α-ZrP from acidic solutions showed promising results in terms of selectivity, sorption capacity, kinetics and reusability. Therefore, α-ZrP was packed as the stationary phase in a column and its ability to separate Sc(III) and Fe(III) was assessed. At first, a breakthrough curve was constructed with the Sc(III)/Fe(III) binary solution as feed (Figure 12). The synthetic solution was prepared by mimicking the Sc/Fe concentration ratio of a typical BR acidic leachate.

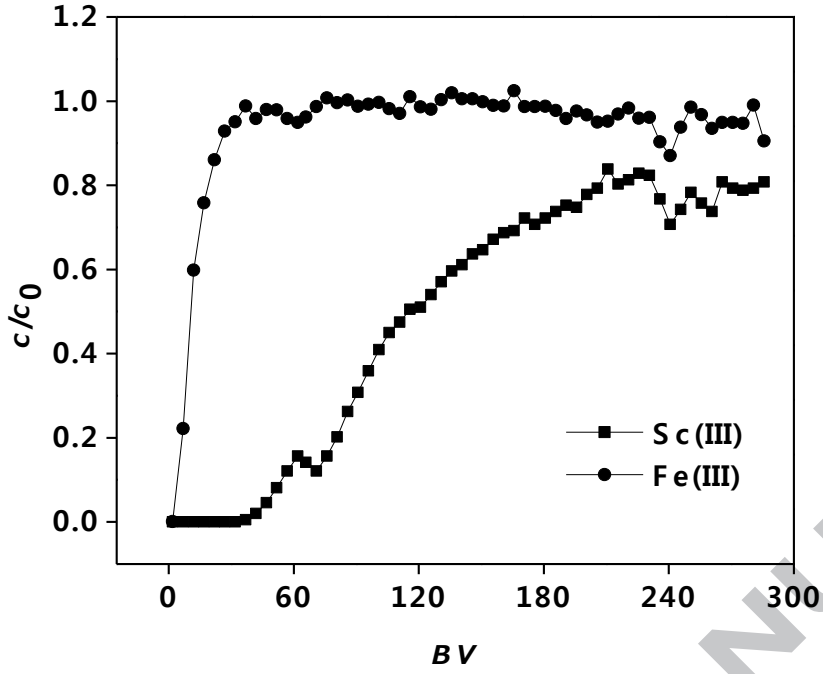

Figure 12. Breakthrough curve of Sc(III) and Fe(III) from binary HCl solution (pH_{ini} = 0.8). Feed: 0.04 mmol L^{-1} of Sc(III), Fe/Sc molar ratio = 43. Flow rate 2 *BV* h^{-1}.

Under acidic conditions, Fe(III) started to break through at 1 *BV*, while Sc(III) break through at 32 *BV*, confirming the remarkable selectivity of α-ZrP for Sc(III). The sorption performance of Sc(III) through the column could be analysed by the established mathematical models: Thomas, Yoon-Nelson or Adams-Bohart model [61]. Since it has been confirmed batchwise that Sc(III) uptake by the α-ZrP follows Langmuir isotherm model and the pseudo-second-order reaction, it might seem reasonable to attempt fitting the data to the Thomas model. However, our dual metal loading process did not fit well with the Thomas model since the Sc(III) and Fe(III) are essentially competing with each other during the loading. Nevertheless, the breakthrough study revealed the potential applicability of α-ZrP for Sc(III) recovery and purification from BR leachates.

As a demonstration, a freshly prepared HCl BR leachate, without any further pH adjustments, was loaded onto the α-ZrP column. Although the Sc(III) concentration in the leachate was low (2 mg L^{-1}), it was completely recovered (>99.9%) by α-ZrP, even in the presence of the highly concentrated base elements (Table 4).

Table 4. Composition of the HCl BR leachate and recovery of elements by the α-ZrP.

Elements	Concentration in the leachate (mg L^{-1})	Recovery (%) by the α-ZrP
Ca	5108	6.2
Al	2653	3.9
Si	1202	35.2
Fe	358	54.1
Ti	227	43.3
Ce	9.9	21.7
La	9.3	15.6
Nd	3.7	38.6
Sc	1.9	>99.9
Y	1.7	29.2
Dy	0.6	8.9

However, certain amounts of base elements, and especially of Fe(III) (54.1%), were recovered by α-ZrP along with Sc(III). In order to separate Sc(III) and other co-loaded elements, a simple concentration gradient elution with HCl was performed (Figure 13). The majority of elements

recovered by the α-ZrP from the BR leachate break through at the first *BV* and were nearly completely eluted with 1 mol L^{-1} HCl at 31 *BV*. However, 40% of Sc(III) was eluted at 31 *BV*. Therefore, Sc(III) elution was enhanced by 2 mol L^{-1} HCl and it was completely eluted at 48 BV. About 60% of Sc(III) was eluted with 2 mol L^{-1} HCl in the last 17 BV. In these Sc(III) fractions no Fe(III), Al(III), Ca(II) or other REEs impurities were detected, resulting in a remarkable separation from other elements of the remaining 60% of Sc(III). The performed procedure outstands the previous studies on Sc(III) recovery form BR leachates by its simplicity, effectiveness and scandium purity [27,62]. When considering the fact that the BR leachate was obtained under non-optimised conditions and was tested without any further treatment, the results indicate that α-ZrP may offer a unique possibility for obtaining high purity scandium from BR leachates. The finally performed elution chromatography experiment represents a successful proof-of-principle to selectively recover and purify Sc(III) from a real BR leachate by α-ZrP.

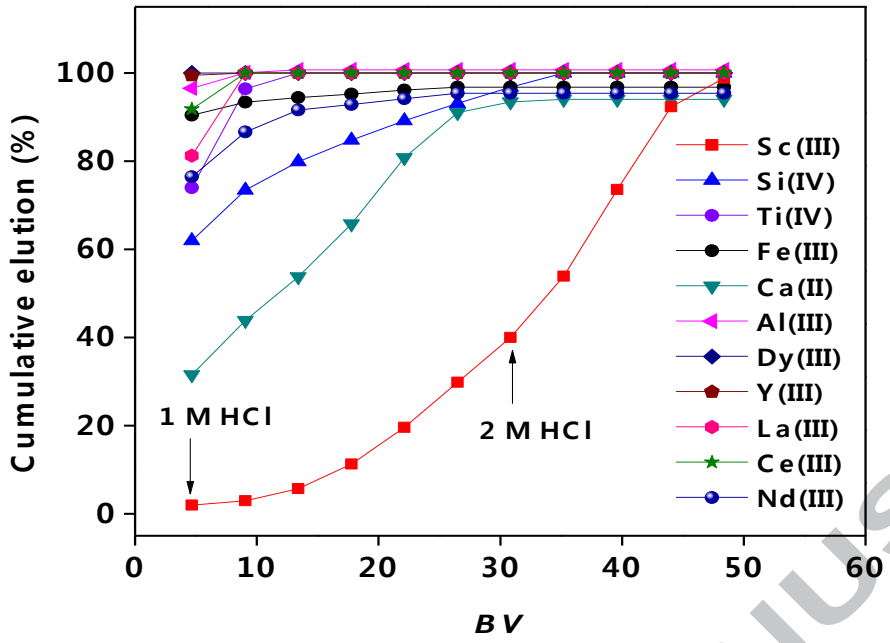

Figure 13. Cumulative elution of elements recovered by α-ZrP from BR HCl leachate. Eluent: 1-2 mol L^{-1} HCl. Feed: pH_{ini} = 2.2, V = 5 mL, flow rate 2 BV h^{-1}.

4. CONCLUSIONS

α-ZrP materials possess excellent selectivity towards Sc(III) in the presence of high concentrations of Fe(III) and other base elements. This interesting feature indicates potential to apply these materials in the separation of Sc(III) and Fe(III) from BR leachates, as these elements exhibit similar properties and thus their separation is generally difficult. Among the tested materials (α-ZrP, am-ZrP, α-TiP, am-TiP), α-ZrP exhibited the highest Sc(III)/Fe(III) separation factors (up to 23). Hydration enthalpy, ionic radii, crystallinity of the material and the pH of the solution were found to be the dominant factors that have an influence on the α-ZrP selectivity for Sc(III). α-ZrP exhibited very fast kinetics for Sc(III) uptake of 15 minutes, which indicated a practical applicability of the ion exchanger for column chromatography processes.

Furthermore, the applicability of α-ZrP was verified in a chromatography column by loading BR leachate with 0.7 mol L^{-1} HCl, without any pretreatment. Most elements were not recovered by α-ZrP, whereas the recovery of Sc(III) was complete (>99.99%). Moreover, by elution with 2 mol L^{-1} HCl, 60% of the recovered Sc(III) could be separated well from the base elements and other REEs in BR. High-purity Sc(III) fractions were obtained after a single chromatography separation. In conclusion, α-ZrP is highly effective in purification of Sc(III) from very complex matrices, such as a leachate of BR.

5. CONFLICTS OF INTEREST

There are no conflicts to declare.

6. ACKNOWLEDGMENTS

The research leading to these results has received funding from the European Community's Horizon 2020 Programme under Grant Agreement number 636876 (REDMUD – H2020-MSCA-ITN-2014). Project website: etn.redmud.org. Tobias Hertel is thanked for XRD measurements and Sami Hietala for NMR.

7. REFERENCES

[1] K. Binnemans, P.T. Jones, T. Müller, L. Yurramendi, Rare Earths and the Balance Problem: How to Deal with Changing Markets?, J. Sustain. Metall. 4 (1) (2018) 126–146.

[2] S. Badwal, Scandia–zirconia electrolytes for intermediate temperature solid oxide fuel cell operation, Solid State Ionics 136-137 (1–2) (2000) 91–99.

[3] J. Zhang, B. Zhao, B. Schreiner, Separation Hydrometallurgy of Rare Earth Elements, Springer International Publishing, Cham, Switzerland, 2016.

[4] Z. Ahmad, The properties and application of scandium-reinforced aluminum, JOM 55 (2) (2003) 35–39.

[5] S. Das, S.S. Behera, B.M. Murmu, R.K. Mohapatra, D. Mandal, R. Samantray, P.K. Parhi, G. Senanayake, Extraction of scandium(III) from acidic solutions using organo-phosphoric acid reagents: A comparative study, Sep. Purif. Technol. 202 (2018) 248–258.

[6] A. Bauer, US Patent US3351798A (1963).

[7] C. M. David, P. Gupta, Lasers in Dentistry: A Review, Int. J. Adv. Health Sci. 2 (8) (2015) 7–13.

[8] J. Röyset, Scandium in aluminium alloys overview: physical metallurgy, properties and applications, Metall. Sci. Techn. 25 (2007) 12–21.

[9] W. Wang, Y. Pranolo, C.Y. Cheng, Metallurgical processes for scandium recovery from various resources: A review, Hydrometallurgy 108 (1–2) (2011) 100–108.

[10] European Commission, Ad hoc Working Group on defining critical raw materials, Report on Critical Raw Materials for the EU (2014).

[11] European Commission, Directorate-General for Internal Market, Industry, Entrepreneurship and SMEs, Study on the review of the list of Critical Raw Materials: executive summary (2017).

[12] J. Vind, A. Malfliet, B. Blanpain, P. Tsakiridis, A. Tkaczyk, V. Vassiliadou, D. Panias, Rare Earth Element Phases in Bauxite Residue, Minerals 8 (2) (2018) 77 (1–32).

[13] C.R. Borra, Y. Pontikes, K. Binnemans, T. Van Gerven, Leaching of rare earths from bauxite residue (red mud), Min. Eng. 76 (2015) 20–27.

[14] R.P. Narayanan, L.-C. Ma, N.K. Kazantzis, M.H. Emmert, Cost Analysis as a Tool for the Development of Sc Recovery Processes from Bauxite Residue (Red Mud), ACS Sustain. Chem. Eng. 6 (4) (2018) 5333–5341.

[15] R.P. Narayanan, N.K. Kazantzis, M.H. Emmert, Selective Process Steps for the Recovery of Scandium from Jamaican Bauxite Residue (Red Mud), ACS Sustain. Chem. Eng. 6 (1) (2017) 1478–1488.

[16] R.M. Rivera, B. Ulenaers, G. Ounoughene, K. Binnemans, T. Van Gerven, Extraction of rare earths from bauxite residue (red mud) by dry digestion followed by water leaching, Min. Eng. 119 (2018) 82–92.

[17] R.M. Rivera, G. Ounoughene, C.R. Borra, K. Binnemans, T. Van Gerven, Neutralisation of bauxite residue by carbon dioxide prior to acidic leaching for metal recovery, Min. Eng. 112 (2017) 92–102.
[18] L. Piga, F. Pochetti, L.J. Stoppa, Recovering metals from red mud generated during alumina production, JOM (45) (1993) 54–59.
[19] K. Hammond, B. Mishra, D. Apelian, B. Blanpain, CR3 Communication: Red Mud – A Resource or a Waste?, JOM 65 (3) (2013) 340–341.
[20] C.R. Borra, B. Blanpain, Y. Pontikes, K. Binnemans, T. Van Gerven, Smelting of Bauxite Residue (Red Mud) in View of Iron and Selective Rare Earths Recovery, J. Sustain. Metall. 2 (1) (2016) 28–37.
[21] C.R. Borra, B. Blanpain, Y. Pontikes, K. Binnemans, T. Van Gerven, Recovery of Rare Earths and Major Metals from Bauxite Residue (Red Mud) by Alkali Roasting, Smelting, and Leaching, J. Sustain. Metall. 3 (2) (2017) 393–404.
[22] C.R. Borra, B. Blanpain, Y. Pontikes, K. Binnemans, T. Van Gerven, Recovery of Rare Earths and Other Valuable Metals From Bauxite Residue (Red Mud): A Review, J. Sustain. Metall. 2 (4) (2016) 365–386.
[23] W. Wang, Y. Pranolo,C.Y. Cheng, Recovery of scandium from synthetic red mud leach solutions by solvent extraction with D2EHPA, Sep. Purif. Techn. 108 (2013) 96–102.
[24] B. Onghena, C.R. Borra, T. Van Gerven, K. Binnemans, Recovery of scandium from sulfation-roasted leachates of bauxite residue by solvent extraction with the ionic liquid betainium bis(trifluoromethylsulfonyl)imide, Sep. Purif. Techn. 176 (2017) 208–219.
[25] J. Roosen, S. van Roosendael, C.B. Borra, T. Van Gerven, S. Mullens, K. Binnemans, Recovery of scandium from leachates of Greek bauxite residue by adsorption on functionalized chitosan–silica hybrid materials, Green Chem. 18 (7) (2016) 2005–2013.
[26] M. Ochsenkühn-Petropulu, Th. Lyberopulu, G. Parissakis, Selective separation and determination of scandium from yttrium and lanthanides in red mud by a combined ion exchange/solvent extraction method, Anal. Chim. Acta 315 (1–2) (1995) 231–237.
[27] W. Zhang, R. Koivula, E. Wiikinkoski, J. Xu, S. Hietala, J. Lehto, R. Harjula, Efficient and Selective Recovery of Trace Scandium by Inorganic Titanium Phosphate Ion-Exchangers from Leachates of Waste Bauxite Residue, ACS Sustain. Chem. Eng. 5 (4) (2017) 3103–3114.
[28] D. Depuydt, W. Dehaen, K. Binnemans, Solvent Extraction of Scandium(III) by an Aqueous Biphasic System with a Nonfluorinated Functionalized Ionic Liquid, Ind. Eng. Chem. Res. 54 (36) (2015) 8988–8996.
[29] L. Schmidt, J.S. Fritz, Ion-exchange preconcentration and group separation of ionic and neutral organic compounds, J. Chromatogr. A 640 (1–2) (1993) 145–149.
[30] Inamuddin, M. Luqman, Ion exchange technology, Springer, Dordrecht, The Nederlands 2012.

[31] H. Mohammedi, H. Miloudi, A. Tayeb, C. Bertagnolli, A. Boos, Study on the extraction of lanthanides by a mesoporous MCM-41 silica impregnated with Cyanex 272, Sep. Purif. Techn. 209 (2019) 359–367.
[32] X. Sun, B. Peng, Y. Ji, J. Chen, D. Li, The solid–liquid extraction of yttrium from rare earths by solvent (ionic liquid) impreganated resin coupled with complexing method, Separation and Purification Technology 63 (1) (2008) 61–68.
[33] E. Ferizoglu, Ş. Kaya, Y. A. Topkaya, Solvent extraction behaviour of scandium from lateritic nickel-cobalt ores using different organic reagents, Physicochem. Probl. Miner. Process. 54 (2) (2018) 538-545.
[34] Derek W. Smith, ionic hydration enthalpies, J. Chem. Educ. 54 (9) (1977) 540–542.
[35] D. Avdibegović, M. Regadío, K. Binnemans, Recovery of scandium(III) from diluted aqueous solutions by a supported ionic liquid phase (SILP), RSC Adv. 7 (78) (2017) 49664–49674.
[36] G. Alberti, Syntheses, crystalline structure, and ion-exchange properties of insoluble acid salts of tetravalent metals and their salt forms, Acc. Chem. Res. 11 (1978) 163-170.
[37] B.F. Alfonso, C. Trobajo, M.A. Salvadó, P. Pertierra, S. García-Granda, J. Rodríguez-Fernández, J.A. Blanco, J.R. García, Synthesis and Characterization of α-Titanium Phosphate/Propylamine Intercalation Compounds Containing Transition-Metal Ions, Z. anorg. allg. Chem. 631 (11) (2005) 2174–2180.
[38] H. Xiao, W. Dai, Y. Kan, A. Clearfield, H. Liang, Amine-intercalated α-zirconium phosphates as lubricant additives, Appl. Surf. Sci. 329 (2015) 384–389.
[39] A. Díaz, V. Saxena, J. González, A. David, B. Casañas, C. Carpenter, J.D. Batteas, J.L. Colón, A. Clearfield, M.D. Hussain, Zirconium phosphate nano-platelets: A novel platform for drug delivery in cancer therapy, Chem. Commun. (Camb.) 48 (12) (2012) 1754–1756.
[40] C. Bisio, M. Nocchetti, F. Leroux, Recent developments in intercalation compounds: Chemistry and applications, Dalton Trans. 47 (9) (2018) 2838–2840.
[41] A. Clearfield, Inorganic ion exchange materials, CRC Press, Boca Raton, Florida, 1982.
[42] W. W. Rudolph, C. C. Pye, Aqueous Solution Chemistry of Scandium(III) Studied by Raman Spectroscopy and ab initio Molecular Orbital Calculations, J. Solution Chem. 29 (2000) 955–986.
[43] A. Stefánssona, Kono H. Lemkeb, Terry M. Sewardc, In: Proc. 15th International Conference on the Properties of Water and Steam, 8–11 September, Berlin, Germany, 2008.
[44] B. Pan, Q. Zhang, W. Du, W. Zhang, B. Pan, Q. Zhang, Z. Xu, Q. Zhang, Selective heavy metals removal from waters by amorphous zirconium phosphate: Behavior and mechanism, Water Res. 41 (14) (2007) 3103–3111.
[45] A. Clearfield, W. L. Duax, A. S. Medina, G, D. Smith, J. R. Thomas, Mechanism of ion exchange in crystalline zirconium phosphates. I. Sodium ion exchange of α-zirconium phosphate, J. of Phys. Chem. 73 (10) (1969) 3424–3430.

[46] J. Xu, E. Wiikinkoski, R. Koivula, W. Zhang, B. Ebin, R. Harjula, HF-Free Synthesis of α-Zirconium Phosphate and Its Use as Ion Exchanger for Separation of Nd(III) and Dy(III) from a Ternary Co–Nd–Dy System, J. Sustain. Metall. 3 (3) (2017) 646–658.
[47] B.M. Mosby, A. Díaz, V. Bakhmutov, A. Clearfield, Surface functionalization of zirconium phosphate nanoplatelets for the design of polymer fillers, ACS applied materials & interfaces 6 (1) (2014) 585–592.
[48] J. Xu, R. Koivula, W. Zhang, E. Wiikinkoski, S. Hietala, R. Harjula, Separation of cobalt, neodymium and dysprosium using amorphous zirconium phosphate, Hydrometallurgy 175 (2018) 170–178.
[49] A. Clearfield, J. Stynes, The preparation of crystalline zirconium phosphate and some observations on its ion exchange behaviour, J. Inorg. Nucl. Chem. 26 (1) (1964) 117–129.
[50] L. Sun, W.J. Boo, H.-J. Sue, A. Clearfield, Preparation of α-zirconium phosphate nanoplatelets with wide variations in aspect ratios, New J. Chem. 31 (1) (2007) 39–43.
[51] A. Clearfield, G.D. Smith, Crystallography and structure of .alpha.-zirconium bis(monohydrogen orthophosphate) monohydrate, Inorganic chemistry 8 (3) (1969) 431–436.
[52] B.M. Mosby, A. Díaz, V. Bakhmutov, A. Clearfield, Surface functionalization of zirconium phosphate nanoplatelets for the design of polymer fillers, ACS Appl. Mater. Interfaces 6 (1) (2014) 585–592.
[53] R. Thakkar, U. Chudasama, Synthesis and characterization of zirconium titanium phosphate and its application in separation of metal ions, J. Hazard. Mater. 172 (1) (2009) 129–137.
[54] G. Alberti, E. Torracca, A. Conte, Stoicheiometry of ion exchange materials containing zirconium and phosphate, J. Inorg. Nucl. Chem. 28 (2) (1966) 607–613.
[55] R.D. Shannon, Revised effective ionic radii and systematic studies of interatomic distances in halides and chalcogenides, Acta Cryst. A 32 (5) (1976) 751–767.
[56] W. Song, M.A. Larson, Activity coefficient model of concentrated electrolyte solutions, AIChE Journal 36 (12) (1990) 1896–1900.
[57] Z. Zhao, Y. Baba, W. Yoshida, F. Kubota, M. Goto, Development of novel adsorbent bearing aminocarbonylmethylglycine and its application to scandium separation, J. Chem. Technol. Biotechnol. 91 (11) (2016) 2779–2784.
[58] N. Van Nguyen, A. Iizuka, E. Shibata, T. Nakamura, Study of adsorption behavior of a new synthesized resin containing glycol amic acid group for separation of scandium from aqueous solutions, Hydrometallurgy 165 (2016) 51–56.
[59] H. Paudyal, B. Pangeni, K. Nath Ghimire, K. Inoue, K. Ohto, H. Kawakita, S. Alam, Adsorption behavior of orange waste gel for some rare earth ions and its application to the removal of fluoride from water, Chem. Eng. J. 195–196 (2012) 289–296.
[60] J. Ma, Z. Wang, Y. Shi, Q. Li, Synthesis and characterization of lysine-modified SBA-15 and its selective adsorption of scandium from a solution of rare earth elements, RSC Adv. 4 (78) (2014) 41597–41604.

[61] Z.Z. Chowdhury, S.M. Zain, A.K. Rashid, R.F. Rafique, K. Khalid, Breakthrough Curve Analysis for Column Dynamics Sorption of Mn(II) Ions from Wastewater by Using Mangostana garcinia Peel-Based Granular-Activated Carbon, J. Chem. 2013 (5) (2013) 1–8.
[62] D. Avdibegović, M. Regadío, K. Binnemans, Efficient separation of rare earths recovered by a supported ionic liquid from bauxite residue leachate, RSC Adv. 8 (22) (2018) 11886–11893.

Highlights

- Zirconium phosphate possesses excellent selectivity towards Sc(III).
- The sorption capacity of zirconium phosphate for Sc(III) is remarkable.
- Direct separation of Sc(III) and Fe(III) by zirconium phosphate was achieved.
- High-purity Sc(III) fractions were obtained from bauxite residue leachates.
- This method holds great potential for the recovery of Sc(III) from bauxite residue.

Graphical abstract